

## TOWARDS NON-PERMANENT CONTACTING SCHEMES FOR BUSBAR-FREE SOLAR CELLS

Axel Herguth<sup>1</sup>, Stefan Braun<sup>1</sup>, Giso Hahn<sup>1</sup>, Christoph Poenisch<sup>2</sup>, Robin Nissler<sup>2</sup>

<sup>1</sup>University of Konstanz, Department of Physics, 78457 Konstanz, Germany

<sup>2</sup>Gebr. Schmid GmbH & Co, Robert-Bosch-Str. 32-34, 72250 Freudenstadt, Germany

**ABSTRACT:** The multi-busbar solar cell concept using a multitude of wires instead of few busbars is a promising candidate for large scale industrial application for several reasons: it can be combined with the probably upcoming dielectrically passivated back side (PERC) and bifacial concepts, uses less silver and allows for smaller fill factor losses when embedded in a module. However, the electrical characterization of this cell type is not straightforward as the metallization consists prior to module integration only of the finger grid and the commonly contacted busbars are missing. In this contribution several alternative approaches for non-permanent electrical contacting of busbar-free solar cells are described as the commonly used 'external busbars' method is found to overestimate series resistance and thus underestimates fill factor and conversion efficiency. The electrical properties of the setups are evaluated and the advantages and disadvantages are compared. In the end one concept is found to work sufficiently well.

**Keywords:** Characterization, Electrical Properties, Busbar-free Solar Cells

### 1 INTRODUCTION

Today's standard industrial solar cells still feature a (quasi) one-dimensional structure with a vertical pn-junction and bifacial metallization. In most cases an H-pattern scheme (a multitude of fingers inter-connected by two or three perpendicular busbars) is used for the front contact, allowing for a reliable soldering on the one hand and an acceptable shading on the other hand.

But the H-pattern metallization scheme on the front side of the cell imposes three major limitations to the solar cell. First, it causes low, but still significant shading and thus a lower current generation. Second, the length of the fingers accounts for a significant part of the device's series resistance limiting the fill factor and thus the conversion efficiency. Third, the commonly used silver is responsible for a significant part of the solar cell's production cost [1,2].

Unfortunately, these limitations cannot be optimized independently in an H-pattern: thinner fingers lower the shading and the silver costs but most likely increase the series resistance and thus lower fill factor and efficiency.

Due to these restrictions several institutes and companies have begun to develop two-stage metallization concepts [3,4] that in the first stage comprise only of a 'classical' grid of parallel, not-interconnected fingers yielding only an unusable busbar-free solar cell precursor. Then in a second step a multitude of wires or alike are soldered or glued perpendicular to the fingers prior or even within the stringing or module lamination process which then allow for current extraction. Day4Energy used this metallization scheme as of 2005/2006 [3]. Promising results have been published for these concepts showing higher currents while maintaining a high fill factor even in the module [4].

However, a massive drawback of these metallization concepts is that a proper electrical characterization of the busbar-free cell is hardly feasible prior to soldering or gluing. Unfortunately, this characterization is required for a reasonable classification prior to module integration. Proper classification therefore requires a non-permanent contacting setup capable of measuring the busbar-free cell as close to the module situation as possible.

In this contribution several approaches for non-permanent contacting schemes and their individual electrical and optical properties are described and the advantages and disadvantages are discussed.

### 2 PROPERTIES OF THE BUSBAR-FREE CELL

The metallization scheme of busbar-free solar cells consists only of non-interconnected narrow fingers. The exact number depends on the emitter sheet resistance. In the following, 86 fingers (1.8 mm spaced) are used which are spread equidistantly on the 156×156 mm<sup>2</sup> full-square cell. The fingers are screen-printed or built up in a seed-and-plate manner. It should be noted that the finger's effective height may differ by several microns due to local variations in wafer thickness as well as process inhomogeneities especially when screen printing techniques are used.

In contrast to solar cells with busbars a multitude of (tin- or indium alloy-coated) copper wires perpendicular to the fingers are used to extract the current from the solar cell. In general, a local variation of the wire diameter or irreversible distortion by several microns cannot be ruled out. The total number of wires depends on its cross-section area and conductivity as well as the fingers conductivity. As simulations have shown, the optimized solar cell features around 10 thick wires for screen-printed silver fingers [4]. However, metallization schemes consisting of three or four times more wires for substrate sizes of 156×156 mm<sup>2</sup> are known to exist.

In the described experiments 15 thin wires were used as their diameter was restricted due to technical restrictions during module lamination.

For the calculation of the series resistance contribution of the finger grid the solar cell can (at least in first approximation) be reduced to a symmetry region with length  $L$  parallel to the fingers from the wire to the centre between two adjacent wires times the inter-finger spacing  $f$ . In our case, the area measures 5.2×1.8 mm<sup>2</sup>. The actual finger length is somewhat shorter than  $L$  but, as the wire diameter (~200 μm compared to 5.2 mm) is assumed to be small, the difference is neglected to simplify calculations.

The length  $L$  can be replaced by the solar cell edge  $L_0$  (156 mm) in order to correlate series resistance with the number  $n$  of used wires:  $L_0 = 2 \cdot n \cdot L$ . The series resistance contribution of the finger grid  $R_f(n)$  is then given by

$$R_f(n) \approx \frac{1}{3} \rho f \frac{L^2}{A} = \frac{1}{12} \rho f \frac{L_0^2}{A \cdot n^2} \quad (1)$$

with specific resistance  $\rho$  and finger cross section  $A$ .

### 3 CONTACTING SCHEMES

#### 3.1 General considerations

The perfect measurement setup should imitate the electrical properties of the situation given in the module. Especially the use of the correct number of front wires, their original conductivity and single sided current extraction is highly recommended if the correct fill factor and I(V) curve is of interest.

The material of the wire is more or less defined by the conductivity of the wire material used in the module being copper with a tin- or indium alloy coating. However, it is not mandatory the same wire as the requirements for the measurement setup are different: the wire has to withstand thousand fold repeated mechanical contact without being inelastically distorted and the surface should be corrosion-free or non-oxidizing. Neither the copper wire nor the tin/indium coating is exceptionally hard, so a harder material like steel or beryllium copper might be a better choice even though the conductivity is smaller and the wire has to be thicker. The additional shading has to be taken into account or has to be compensated. A wire composed of different shells to adjust conductivity and hardness is conceivable.

The surface material can be chosen more or less independently of the wire core. Typical non-oxidizing coating materials like gold alloys are usable. A certain scratch resistance is advisable to guarantee a long service life in mass production.

For laboratory use and for the setups shown later on a gold-plated copper wire was found to work sufficiently well. However, special care should be taken on the straightness of the wire as the waviness adds up to the effective finger height as discussed later.

The electrical contact has to be non-permanent, non-soiling and non-destructive, so the contact to the fingers may be achieved only by the physical contact. Assuming clean surfaces of both finger and wire, the quality of the contact is mainly defined by the force pressing the wire onto the finger which has to exceed a certain threshold value. One should notice that in our case there are  $86 \times 15 = 1290$  contact sites present, and that almost all sites should be contacted correctly.

#### 3.2 State of the Art: ‘External busbars’

The approach to probably think about first is to use some kind of external busbars simply pressed onto the busbar-free solar cell. Day4Energy presented such an approach recently [5]. Within this approach the contact to each finger is made by a wire which is mounted under an elastic material or spring-loaded under a stiff bridge. However, this kind of setup can be quite cumbersome and causes non-negligible shading. Hence only few bridges  $m$  are usable even though the finger grid was designed and optimized for a certain number  $n$  of wires. This causes a finger related series resistance mismatch between the apparent, measured resistance  $R_f(m)$  and the actual resistance  $R_f(n)$  according to Eq. 1

$$\frac{R_f(m)}{R_f(n)} = \frac{n^2}{m^2} \quad (2)$$

Eq. 2 is graphically illustrated in Figure 1. The apparent finger related series resistance might exceed the actual value by far. E.g., measuring a solar cell with only three busbars even though it was optimized for fifteen wires increases the apparent finger related series resistance by a factor of twenty-five.

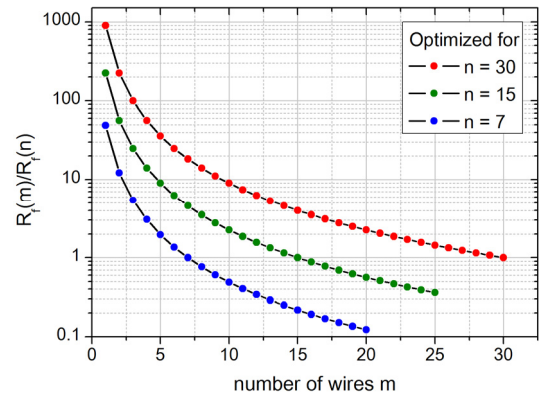


**Figure 1:** Mismatch of the finger related series resistance according to Eq. 2 when the measurement is taken with  $m$  wires, but the design is optimized for  $n$  wires.

In consequence, the fill factor and the conversion efficiency of the solar cell will be systematically underrated. An I(V) characteristic taken with a (strong) series resistance mismatch can hardly be used for analytical purposes, although a rough classification might be possible.

A second effect is difficult to put in formulas. The reduced finger width of the busbar-free design makes it prone to finger interruptions. This disadvantage is widely alleviated when many wires are used as only an interruption between the last wire and the cell's edge can effectively isolate a cell region which is relatively small (max. 5.2 mm for 15 wires). However, when only few wires are used for the measurement, an interruption even far from the edge can isolate large areas (max. 26 mm for 3 wires) and such cells are likely underrated.

In conclusion, this approach cannot always yield the true electrical parameters of the solar cell, and thus the allocation of cells to classes might lead to mismatched modules.

#### 3.3 Bowed ground plate and spring-loaded wires

Within this approach a bowed ground plate is used across which spring-loaded wires are mounted in a frame (Figure 2). When the frame is pressed to the chuck, the wires snuggle to the cell and the contact pressure is due to the wire tension. In our case the bow of the ground plate was chosen to 10 mm. Figure 3 shows an electroluminescence image taken with this setup.



**Figure 2:** Sketch of the bowed ground plate setup. The wire is mounted in a frame between two springs (marked as arrows). If the wire is pushed to the ground plate, the springs allow the wire the necessary elongation and maintain the wire tension so that the wire snuggles to the solar cell (dark grey).

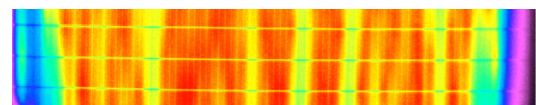


**Figure 3:** Electroluminescence image of a busbar-free solar cell (156 mm across; extract) using the bowed ground plate setup. The wires are running horizontally. The image was taken in strong excitation to grant sensitivity towards series resistance effects.

As can be seen from Figure 3, the homogeneity is insufficient. Especially two effects impede a proper operation. At the edges the EL signal decreases continuously. This behavior is due to the wire taking-off as the height of the frame is not correctly adjusted and the wire tangentially leaves the circular shape of the ground plate still well inside the solar cell. The continuous decrease in signal is then due to the relatively high series resistance within the emitter.

The second effect can be seen in the centre region of the solar cell where some green, low signal lines in direction of the fingers turn up. A closer look on the solar cell revealed a combination of two higher fingers enclosing a lower finger effectively shielding this finger from the wire. Therefore only a certain height difference of the fingers can be tolerated which depends on the bow of the setup (see Figure 4).

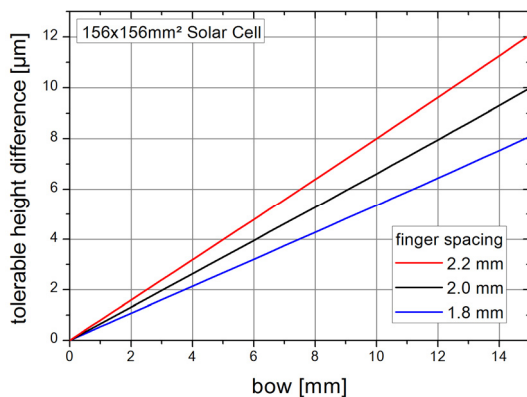


**Figure 4:** Tolerable height difference of the fingers calculated for 156x156 mm<sup>2</sup> solar cells. At differences exceeding the shown value, no proper contact to a lower finger might be achieved.

The intolerance towards effective finger height variation (comprised of wafer thickness, front and rear side metallization, wire diameter and wire waviness) and the required strong bowing of the solar cells are the weaknesses of this concept, and its applicability depends crucially on the uniformity of solar cell thickness and metallization and/or a certain resistance to mechanical stress due to the necessary bowing. A mass production suitable tool seems at least challenging.

Furthermore, the solar cell is no longer mounted flat and thus the optical properties change, e.g., the projected area is smaller than the 'flat' area of the cell. The optical properties of this approach are discussed elsewhere in more detail [6].

### 3.4 Wires covered by flexible foil

In this approach (see Figure 5 top), several wires mounted in a frame are laid across the cell. Above the wires a flexible foil is mounted into the frame in such a way that an air tight chamber between cell and foil is created. The chamber is then evacuated so that the ambient air presses the foil and especially the wires to the cell (Figure 5 bottom).

A luminescence image taken with a down-sized proof-of-principle setup is shown in Figure 6. The achieved homogeneity is promising.

However, in contrast to the methods presented in section 3.2 and 3.3, there is a medium between light source and cell, and it is mandatory to discuss the influence on the measurement.

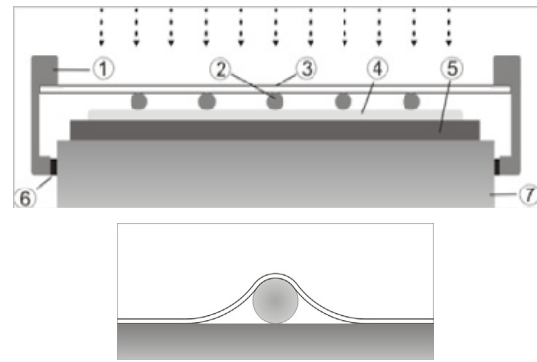


**Figure 5:** (top) Cross-sectional sketch of the setup using wires and a flexible covering foil applied for the electrical characterization of the busbar-free cells. Details: 1 frame, 2 wires, 3 flexible foil, 4 finger, 5 solar cell, 6 airtight seal, 7 chuck; illumination from above. (bottom) The foil is sucked to the cell in between the wires and snuggles to the wires.

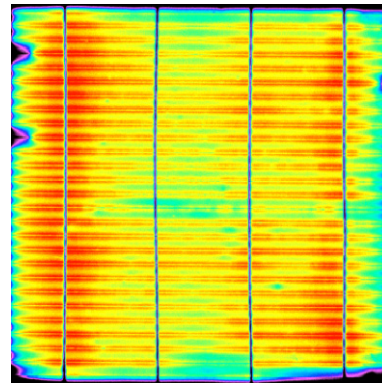


**Figure 6:** Electroluminescence image of a small (5×5 cm<sup>2</sup>) busbar-free solar cell using a flexible foil prototype setup. The wires are running vertically. The image was taken in strong excitation to grant sensitivity towards series resistance effects.

The foil should of course be transparent and free of absorbance, but reflective losses are unavoidable. However, this may be countered by an adjustment of the optical power used for illuminated measurements. The optical properties of this approach are discussed elsewhere in more detail [6].

Although homogeneity in the image of Figure 6: (left) indicates that electrical contact is sufficiently established at most of the contact sites, the approach might not be suited for mass production. Within each contacting cycle the pressure of the ambient stretches the foil, and the foil tends to wear out with time.

Although a flexible mounting of the foil at the edges might compensate this effect, it might also lead to a lateral movement of the foil (and probably the wires) while it snuggles to the surface of the solar cell causing other problems. On the one hand, this movement might damage the surface of the solar cell as the foil locks on locally, e.g., with pyramid tips and silicon cannot withstand shearing forces well. On the other hand, the movement might damage the foil itself as silicon, silicon nitride and metallization (meaning metal as well as glass particles) are probably the harder material, and induces scratch marks in the surface of the foil. This in turn makes the foil dull and opaque with time reducing the current generation if not taken into account.

### 3.5 Wires and an inelastic plate

The setup looks almost the same as for the flexible foil (Figure 5 top), but instead of a foil a thick transparent inelastic plate (e.g., glass or Plexiglas) is mounted above the wires. The inelastic plate has the advantage that the wires can be pressed against each contact site by the weight of the plate/frame or by additional pressure on the frame and that the inelastic plate does not touch the surface of the solar cell. Hence the tight enclosure for the vacuum system is not necessary.

An electroluminescence image taken with a down-sized proof-of-principle setup is shown in Figure 7. The inhomogeneity indicates contacting problems in parts of the solar cell.

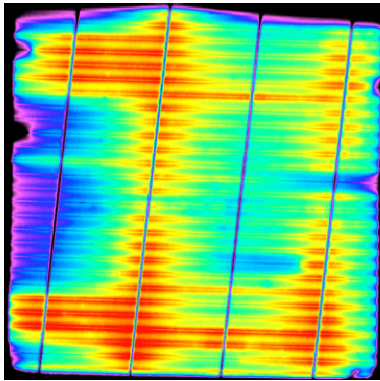


**Figure 7:** Electroluminescence image of a small ( $5 \times 5 \text{ cm}^2$ ) busbar-free solar cell an inelastic plate prototype setup without cavities. The wires are running slightly tilted. The image was taken in strong excitation to grant sensitivity towards series resistance effects. The strong contrast indicates the inhomogeneous pressure on the contact sites.

The undesirable variation of effective finger height can be problematic as an exceptionally high finger not only inhibits a proper contacting in its vicinity but also concentrates the pressure to that point. This effect is observable in Figure 7, where two wires with a red halo (good contact) embed a wire with green halo (insufficient contact).

### 3.6 Wires, inelastic plate with cavities (and vacuum)

To avoid problems with the effective finger height the wires have to be spring-loaded on their full length and therefore a cavity in the inelastic plate has been introduced which is filled with an elastic material (see Figure 8). If too much pressure is applied to a certain point, the wire is pressed elastically into the cavity and thus buffers the unwanted pressure. Besides the elastic bearing of the wires the cavities also act as guidance for the wires and thereby avoid the lateral slipping of the wires. In the setups without guiding cavities this effect was suppressed by increased wire tension; however, a complete avoidance failed.

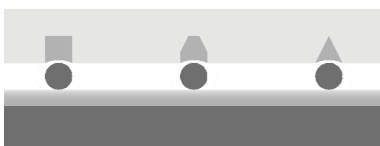


**Figure 8:** Different shapes of the cavity driven into the inelastic plate. The effective shading of the wire beneath can be manipulated from full on the left to almost zero on the right.

Furthermore, the geometrical shape of the cavity allows for a regulation of the effective shading of the wire beneath (Figure 8). If an angled wall of the cavity is used, light actually incident on the cavity can be deflected to the solar cell. This effect can be enhanced by applying a reflective coating to the cavity walls or choosing the angle in such way that total reflection occurs. However, leaving a horizontal part (Figure 8, middle) still allows for a complete shading and thus engineering of a virtual wire width. This can be used, for example, to reduce the virtual wire width to the width of the copper wires used in the module although the actual non-copper wire had to be chosen thicker in order to guarantee the correct conductivity. The optical properties of this approach are discussed elsewhere in more detail [6].

The resulting setup looks still almost as the setup shown in Figure 5 (top) but instead of a foil a thick transparent inelastic plate (e.g., glass or Plexiglas) is mounted above the wires with cavities driven into the plate as shown in Figure 8.

It has been found that the weight of the frame and plate might not be sufficient to guarantee a contact at every contact site as the weight is distributed on a multitude of sites and the wire has to be pushed into the cavities at exposed sites. Increasing the weight of the frame or even putting additional pressure (e.g., pneumatically) on it, might be a way to improve the situation. However, it has also been observed that too much pressure on the edges of the plate can flex even a thick inelastic plate (e.g., glass) by a few dozen microns as the outer fingers act as pivotal lines. In consequence, too much pressure or weight can lead to the situation that contact sites in the center of the solar cell are virtually free of pressure and no electrical contact is established at all.

A simple but well working solution for this problem is to use a plate thick enough to guarantee that almost no flexing occurs. This solution has also the advantage that the weight of the plate increases and thus generally less pressure on the frame is required. From an optical point of view the thickness of the transparent plate made of widely non-absorbing material is often not the limiting factor as the main losses in transmittance are due to reflection at the surfaces. However, the disadvantage at least for lab-type application of this solution is that the setup becomes cumbersome and manual handling becomes challenging. Therefore another approach was chosen.

A second, more advanced solution is to combine the inelastic plate setup with the vacuum system present in the flexible foil setup (Figure 5 top). This yields a more homogeneous pressure distribution which is beneficial to contact homogeneity. An electroluminescence image taken with this kind of setup is shown in Figure 9.

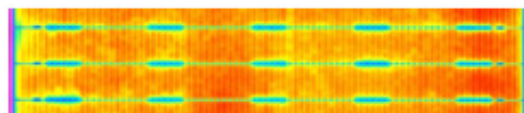


**Figure 9:** Electroluminescence image of a busbar-free solar cell (156 mm across, extract) using the inelastic plate/vacuum setup. The wires are running horizontally. The image was taken in strong excitation to grant sensitivity towards series resistance effects.

As can be seen, a fairly good homogeneity is achieved, and even the five soldering pads printed with silver-aluminum paste instead of aluminum paste at the back side of the cell can be clearly identified.

#### 4. CONCLUSIONS

The electrical characterization of busbar-free solar cells is not straightforward. The already used approach featuring ‘external busbars’ pressed to the cell is in our opinion incapable of determining the correct electrical parameters without corrections as the series resistance of the finger grid is systematically overestimated.

Several alternative setups for the correct measurement of busbar-free solar cells were constructed. The advantages and disadvantages of the different setups were evaluated primarily by electroluminescence imaging as this technique is sensitive to (finger related) series resistance under strong excitation and allows for a spatially resolved analysis.

The analysis showed that the setup with a bowed ground plate and spring loaded wires as well as the setup with an inelastic plate (without cavities) were incapable of establishing a proper electrical contact at the majority of the contact sites (Figure 3; Figure 7). Even though this might be (partly) due to mechanical imperfections of the used setups, especially variations in the effective height of the finger (consisting of variations in substrate thickness, finger height and wire diameter) systematically impede the physical contact of the used wires and the fingers. Therefore these approaches are seen as inappropriate.

Only the vacuum supported flexible foil setup as well as the vacuum supported inelastic plate with cavities setup yielded reasonable results (Figure 6; ; Figure 9). Due to the elastic bearing of the wires both systems guarantee a certain pressure at each contact site and thus the electrical contact is established at the majority of contact sites.

However, as the flexible foil is pressed onto the cell by the ambient, it is stretched in each contacting cycle and tends to wear out with time. In addition it might touch the solar cell’s textured surface in between the fingers and might sustain scratches with time making the foil dull and opaque. In contrast the approach featuring an inelastic plate (like glass) with cavities filled with elastic material to guide and spring the contact wires is likely to be more long lasting and in addition allows for a control of wire shadowing by shaping the cavities in a distinct manner. This approach has been filed for patent application.

#### 5. REFERENCES

- [1] S. Braun et al., *Proc. 22<sup>nd</sup> Workshop on crystalline Silicon Solar Cells & Modules: Materials and Processes*, Vail, CO, p. 18, 2012
- [2] S. Braun et al.; *to be published in J.PV.*
- [3] A. Schneider et al., *Proc. 4<sup>th</sup> WCPEC*, Waikoloa, 2006, p. 1095.
- [4] S. Braun et al., *Energy Procedia* **27** (2012), 227.
- [5] R. Grischke et al., *Proc. 26<sup>th</sup> EU-PVSEC*, 2011, p.1558, 2BV.2.48
- [6] Herguth et al., *to be published*